



## **Molecular tectonics: enantiomerically pure chiral crystals based on trans -1,2-cyclohexanediol**

Benjamin Forquin, Julien Berthaud, Abdelaziz Jouaiti, Nathalie Kyritskas, Sylvie Ferlay, Mir Wais Hosseini

### **► To cite this version:**

Benjamin Forquin, Julien Berthaud, Abdelaziz Jouaiti, Nathalie Kyritskas, Sylvie Ferlay, et al.. Molecular tectonics: enantiomerically pure chiral crystals based on trans -1,2-cyclohexanediol. CrystEngComm, 2019, 21 (34), pp.5129-5136. <10.1039/c9ce00807a>. <hal-02301848>

**HAL Id: hal-02301848**

**<https://hal.science/hal-02301848v1>**

Submitted on 30 Nov 2020

**HAL** is a multi-disciplinary open access archive for the deposit and dissemination of scientific research documents, whether they are published or not. The documents may come from teaching and research institutions in France or abroad, or from public or private research centers.

L'archive ouverte pluridisciplinaire **HAL**, est destinée au dépôt et à la diffusion de documents scientifiques de niveau recherche, publiés ou non, émanant des établissements d'enseignement et de recherche français ou étrangers, des laboratoires publics ou privés.



HAL Authorization

## ARTICLE

Molecular tectonics: enantiomerically pure chiral crystals based on *trans*-1,2-cyclohexanediolBenjamin Forquin,<sup>a</sup> Julien Berthaud,<sup>a</sup> Abdelaziz Jouaiti,<sup>a\*</sup> Nathalie Kyritskas,<sup>a</sup> Sylvie Ferlay,<sup>a\*</sup> Mir Wais Hosseini<sup>a\*</sup>Received 00th January 20xx,  
Accepted 00th January 20xx

DOI: 10.1039/x0xx00000x

Enantiomerically pure chiral *trans*-1,2-cyclohexanediol ((R,R) or (S,S)) based organic compounds **3b-c** bearing two benzoic acid moieties are self complementary units and thus self-assemble in the crystalline phase into isostructural crystals composed of 1D helical H-bonded networks with opposite handedness. The helical strands form enantiomerically pure triple helices. The racemic mixture of the two chiral ligands **3a** also self-assembles into a 1D achiral H-bonded networks displaying a *zig-zag* type geometry. Upon deprotonation, both chiral **3b** and **3c** bearing two carboxylate moieties behave as coordinating ligands. When combined with Cd(NO<sub>3</sub>)<sub>2</sub> in the presence of ancillary N donor ligands such as Dabco (1,4-Diazabicyclo[2.2.2]octane) or bipy (4,4'-bipyridine), they lead to the formation of enantiomerically pure coordination networks. Whereas for both **Cd-3b-Dabco** and **Cd-3c-Dabco** 1D networks, resulting from the interconnection of 2-2 metallamacrocycles by Dabco behaving as a linear connector, are observed, in the case of 4,4'-Bipy connector (**Cd-3b-Bipy** and **Cd-3c-Bipy**) a 2D coordination network based on the interconnection of binuclear Cd(II) dimers by coordinating ligands and ancillary ligands is generated.

## Introduction

In the last years, due to their potential applications, Chiral Coordination Polymers (CCPs),<sup>1,2,3,4,5</sup> a subclass of CPs<sup>6,7,8</sup> also called MOFs or solid-state porous materials,<sup>9,10</sup> have attracted increasing attention. The rational design and construction of enantiomerically pure coordination polymers still remain challenging, representing an ambitious goal for synthetic chemists. In principle, for the generation of CCPs, three strategies have been developed: (i) combinations of chiral coordinating ligands with metal centres<sup>11,12,13</sup>, (ii) combinations of achiral ligands and metal nodes in a chiral medium (solvent, template, etc)<sup>14</sup>, (iii) combination of achiral components undergoing spontaneous resolution.<sup>15,16,17</sup> For the first strategy, a variety of chiral ligands bearing asymmetric carbon centres, for example,<sup>18,19</sup> or chiral-at-metal metallaligands have been used.<sup>20,21,22,23,24</sup> Chiral CCPs may find applications for enantioselective separation and/or adsorption,<sup>25,26,27,28,29,30,31</sup> asymmetric catalysis,<sup>32,33,34</sup> and sensing.<sup>35</sup> Porous chiral coordination polymers with large channels are of particular interest for the above mentioned applications.<sup>36,37,38,39,40</sup>

For the formation of robust coordination polymers, ligands bearing carboxylate coordinating groups have been widely used, since the diverse coordinating modes they display may lead to interesting networks with various dimensionalities and topologies.<sup>41</sup> The combination of chiral ligands bearing carboxylate coordinating groups has led to the formation of robust CCPs. Along this line, we have designed a pair of new chiral ligands (**3b** and **3c**, see figure 1) bearing benzoic/ate coordinating groups, based on the racemic *trans*-1,2-cyclohexanediol **3a**. Cyclohexanediol may be obtained as pure chiral compound ((R,R) (**1b**- or (S,S)-*trans*-1,2-cyclohexanediol **1c**) as shown in figure 1 or as a racemic mixture (*trans*-1,2-cyclohexanediol, **1a**).

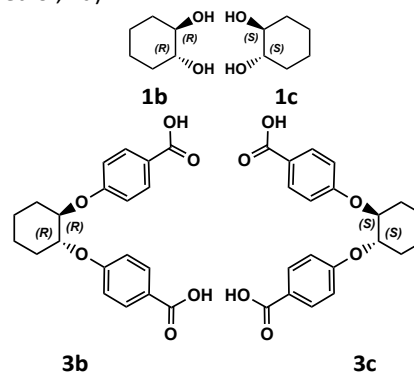


**Figure 1:** Both enantiomers of the chiral *trans*-1,2-cyclohexanediol starting material **1b** and **1c** (top) and the two enantiomerically pure compounds **3b** and **3c** (bottom) bearing two benzoic acids groups. The racemic mixture of the starting materials and of ligands are named **1a** and **3a** respectively.

<sup>a</sup> Molecular Tectonics Laboratory, University of Strasbourg, CNRS, CMC UMR 7140, F-67000 Strasbourg, France

See DOI: 10.1039/x0xx00000x

† Electronic Supplementary Information (ESI) available: XRPD patterns for **3b** and **3c** and TGA traces for **Cd-3b-Dabco** and **Cd-3b-Bipy**.

Chiral compounds **3b** and **3c** (figure 1) are based on chiral (R,R) and (S,S)-*trans*-1,2-cyclohexanediol **1b** and **1c** respectively equipped with two benzoic acid units. An ether junction is used to interconnect the cyclohexyl moiety and benzoic acid units (Figure 1).

The *trans*-cyclohexanediol moieties has already been used as a platform for the design of V-shape ligands bearing two pyridyl units using ester junctions between the chiral scaffold and the coordinating sites. Their combination with ZnSiF<sub>6</sub>, was shown to afford enantiomerically pure crystals, for example.<sup>42</sup>

We report here on the synthesis of two enantiomerically pure compounds based on *trans*-1,2-cyclohexanediol and bearing carboxylic groups, their structural investigation by X-ray diffraction on single crystal and their combinations with Cd(II) cations together with ancillary N donor ligands like Dabco (1,4-Diazabicyclo[2.2.2]octane) or Bipy (4,4'-bipyridine).

## Experimental section

### Characterization techniques

<sup>1</sup>H-NMR and <sup>13</sup>C-NMR spectra were recorded at room temperature on Bruker (400 or 500 MHz) NMR spectrometers by the shared NMR Service of the faculty of chemistry of the Strasbourg University.

Mass spectra (ESI) were recorded on a MicroTOF-Q (Bruker) equipped with an electrospray source.

CD spectra were recorded on a JASCO J-810 spectropolarimeter. Data were collected over a wavelength range of 200-400 nm, at a scan speed of 50 nm/min, bandwidth of 1 nm and data pitch of 0.1 nm. Samples were measured at RT (23 °C) and at given concentrations using a 10 mm path length cuvette (Starna Ltd.) Elemental analyses were performed by the Service de Microanalyses de la Fédération de Recherche Chimie, Université de Strasbourg, Strasbourg, France.

### Synthesis

**General:** All reagents were purchased from commercial sources and used without further purification.

#### Bis-benzonitrile, 4,4'-[*trans*-1,2-cyclohexanediylbis(oxy)] (**2a**, **2b** (1R,2R) and **2c** (1S,2S) )

Under an argon atmosphere, *Trans*-1,2-cyclohexanediol **1a** (or (S,S)-*trans*-1,2-cyclohexanediol **1b** or (R,R)-*trans*-1,2-cyclohexanediol **1c**) (1.0 g, 8.6 mmol) was dissolved in 20 mL of dry DMF. NaH (1.0 g, 25 mmol, 60% dispersion in mineral oil) was added. The reaction was heated at 60 °C for 15 min before 4-fluorobenzonitrile (3.13 g, 25.8 mmol) was added and the reaction mixture was further heated at 120 °C for 48h. The solvent was removed and the crude product was dissolved in 30 mL of CH<sub>2</sub>Cl<sub>2</sub>, the organic phase was washed with aqueous NH<sub>4</sub>Cl (10 %). The organic phase was collected, dried over MgSO<sub>4</sub> and evaporated to dryness. The remaining solid was

purified by flash column chromatography on SiO<sub>2</sub> (CH<sub>2</sub>Cl<sub>2</sub>). The solid was washed twice with MeOH and Et<sub>2</sub>O (10ml) respectively affording compounds **2a**, **2b** and **2c** as white solids in 74, 46 and 61%. Yields respectively.

#### Compound **2a**

<sup>1</sup>H-RMN (400 MHz, CDCl<sub>3</sub>, 25 °C) : δ (ppm) = 7.51 (d, 4H, *J* = 8.8 Hz) ; 6.92 (d, 4H, *J* = 8.8 Hz) ; 4.44 (m, 2H) ; 2.20 (m, 2H) ; 1.83 (m, 2H) ; 1.60 (m, 2H) ; 1.42 (m, 2H);

<sup>13</sup>C-RMN (125 MHz, CDCl<sub>3</sub>, 25 °C) : δ (ppm) = 23.3 ; 29.9 ; 79.2 ; 104.4 ; 116.5 ; 119.3 ; 134.1 ; 161.6.

#### Compound **2b**

<sup>1</sup>H-RMN (400 MHz, CDCl<sub>3</sub>, 25 °C) : δ (ppm) = 7.51 (d, 4H, *J* = 8.8 Hz) ; 6.92 (d, 4H, *J* = 8.8 Hz) ; 4.44 (m, 2H) ; 2.20 (m, 2H) ; 1.83 (m, 2H) ; 1.60 (m, 2H) ; 1.42 (m, 2H);

<sup>13</sup>C-RMN (125 MHz, CDCl<sub>3</sub>, 25 °C) : δ (ppm) = 23.3 ; 29.9 ; 79.2 ; 104.4 ; 116.5 ; 119.3 ; 134.1 ; 161.6.

HRMS (ESI): *m/z* calcd. for C<sub>20</sub>H<sub>18</sub>N<sub>2</sub>O<sub>2</sub> [M-H]: 318.14; found:

#### Compound **2c**

<sup>1</sup>H-RMN (400 MHz, CDCl<sub>3</sub>, 25 °C) : δ (ppm) = 7.51 (d, 4H, *J* = 8.8 Hz) ; 6.92 (d, 4H, *J* = 8.8 Hz) ; 4.44 (m, 2H) ; 2.20 (m, 2H) ; 1.83 (m, 2H) ; 1.60 (m, 2H) ; 1.42 (m, 2H);

<sup>13</sup>C-RMN (125 MHz, CDCl<sub>3</sub>, 25 °C) : δ (ppm) = 23.3 ; 29.9 ; 79.2 ; 104.4 ; 116.5 ; 119.3 ; 134.1 ; 161.6.

#### Bis-benzoic acid, 4,4'-[*trans*-1,2-cyclohexanediylbis(oxy)] (**3a**, **3b** (1R,2R) and **3c** (1S,2S))

An aqueous NaOH solution (62 mmol, 12 mM, 5 mL) was added to a EtOH solution (10 mL) of **2a**, **2b** or **2c** (1g, 3.1 mmol). The mixture was refluxed for 24 h. After evaporation, H<sub>2</sub>O was added (15 mL) and the mixture acidified using an aqueous 37% HCl solution (10 mL). The precipitate thus formed was filtered and washed with H<sub>2</sub>O (2 x 10 mL). After drying under vacuum, pure compounds **3a**, **3b** and **3c** were obtained as white solids in quantitative yield.

#### Compound **3a**

<sup>1</sup>H-RMN (400 MHz, DMSO-d<sub>6</sub>, 25 °C) : δ (ppm) = 12.62 (s, 2H), 7.88 (d, 4H, *J* = 8.8 Hz) ; 7.00 (d, 4H, *J* = 8.8 Hz) ; 4.61 (m, 2H) ; 2.14 (m, 2H) ; 1.70 (m, 2H) ; 1.46 (m, 4H); <sup>13</sup>C-RMN (125 MHz, DMSO-d<sub>6</sub>, 25 °C) : δ (ppm) = 22.8 ; 29.5 ; 78.3 ; 115.2 ; 122.9 ; 131.3 ; 161.5 ; 167.0.

HRMS (ESI): *m/z* calcd. for C<sub>20</sub>H<sub>20</sub>O<sub>6</sub> [M-K]: 395.089; found: 395.087

Anal. Calcd. for C<sub>20</sub>H<sub>20</sub>O<sub>6</sub>: C, 67.4%, H, 5.66%; Found: C, 67.04%, H, 5.52%.

#### Compound **3b**

<sup>1</sup>H-RMN (400 MHz, DMSO-d<sub>6</sub>, 25 °C) : δ (ppm) = 12.62 (s, 2H), 7.88 (d, 4H, *J* = 8.8 Hz) ; 7.00 (d, 4H, *J* = 8.8 Hz) ; 4.61 (m, 2H) ; 2.14 (m, 2H) ; 1.70 (m, 2H) ; 1.46 (m, 4H); <sup>13</sup>C-RMN (125 MHz,

DMSO- $d_6$ , 25 °C) :  $\delta$  (ppm) = 22,8 ; 29,5 ; 78,3 ; 115,2 ; 122,9 ; 131,3 ; 161,5 ; 167,0.

HRMS (ESI):  $m/z$  calcd. for  $C_{20}H_{20}O_6$  [M-K]: 395.089; found: 385.090

Anal. Calcd. for  $C_{20}H_{20}O_6$ : C, 67.41%, H, 5.66%; Found: C, 67.86%, H, 5.45%.

CD spectra see figure 3.

#### Compound **3c**

$^1H$ -RMN (400 MHz, DMSO- $d_6$ , 25 °C) :  $\delta$  (ppm) = 12.62 (s, 2H), 7.88 (d, 4H,  $J$  = 8.8 Hz) ; 7.00 (d, 4H,  $J$  = 8.8 Hz) ; 4.61 (m, 2H) ; 2.14 (m, 2H) ; 1.70 (m, 2H) ; 1.46 (m, 4H);  $^{13}C$ -RMN (125 MHz, DMSO- $d_6$ , 25 °C) :  $\delta$  (ppm) = 22.8 ; 29.5 ; 78.3 ; 115.2 ; 122.9 ; 131.3 ; 161.5 ; 167.0.

HRMS (ESI):  $m/z$  calcd. for  $C_{20}H_{20}O_6$  [M-K]: 395.089; found: 395.087.

Anal. Calcd. for  $C_{20}H_{20}O_6$ : C, 67.41%, H, 5.66%; Found: C, 67.92%, H, 5.37%.

CD spectra see figure 3.

### Crystallisations conditions

A vial containing 0.5 mL of a  $CHCl_3$  solution of **3a**, **3b** or **3c** (5 mg,  $4.55 \times 10^{-3}$  mmol) was placed in a sealed beaker containing  $CH_3OH$ . Slow vapour diffusion at RT of  $CH_3OH$  produced after several days colorless crystals suitable for X-ray diffraction.

#### Cd-3b-dabco or Cd-3c-dabco:

3 mL of a  $H_2O/EtOH$  (1/1) mixture containing compound **3b** (or **3c**) (10 mg,  $28 \times 10^{-3}$  mmol),  $Cd(NO_3)_2$  (6.6 mg,  $28 \times 10^{-3}$  mmol), Dabco (3.2 mg,  $28 \times 10^{-3}$  mmol) and two drops of  $Et_3N$  was placed in a sealed vial. After one week at 100 °C, the crystallization tube was cooled to room temperature affording colourless single crystals.

Due to the presence of different volatile solvents in the crystals, it was not possible to obtain a reliable Elemental Analysis.

#### Cd-3b-Bipy or Cd-3c-Bipy:

3 mL of DMF containing compound **3b** (or **3c**) (10 mg,  $28 \times 10^{-3}$  mmol),  $Cd(NO_3)_2$  (6.6 mg,  $28 \times 10^{-3}$  mmol), bipy (8.7 mg,  $56 \times 10^{-3}$  mmol) was placed in a sealed vial. After two day at 100 °C, the crystallization tube was cooled to room temperature affording colourless single crystals.

Again, due to the presence of different volatile solvents in the crystals, it was not possible to obtain a reliable Elemental Analysis.

### Structural studies

#### Single-Crystal Studies

Data were collected at 173(2) K on a Bruker Apex-II-CCD diffractometer equipped with an Oxford Cryosystem liquid  $N_2$  device, using graphite-monochromated Mo- $K\alpha$  ( $\lambda$  = 0.71073 Å) radiation. For all structures, diffraction data were corrected for absorption. Structures were solved using SHELXS-97 and refined by full matrix least-squares on  $F^2$  using SHELXL-97. The

hydrogen atoms were introduced at calculated positions and refined using a riding model.<sup>43</sup> They can be obtained free of charge from the Cambridge Crystallographic Data Centre via [www.ccdc.cam.ac.uk/datarequest/cif](http://www.ccdc.cam.ac.uk/datarequest/cif). CCDC: 1908303-1908309: 1908303 (**3a**), 1908304 (**3b**), 1908305 (**Cd-3c-Bipy**), 1908306 (**Cd-3b-Bipy**), 1908307 (**3c**), 1908308 (**Cd-3b-dabco**), 1908309 (**Cd-3c-dabco**).

### Powder diffraction studies (PXRD)

Diagrams were collected on a Bruker D8 diffractometer using monochromatic Cu- $K\alpha$  radiation with a scanning range between 4 and 40° using a scan step size of 8°/mn.

As already demonstrated and currently admitted, for all compounds, discrepancies in intensity between the observed and simulated patterns are due to preferential orientations of the microcrystalline powders.

## Results and discussion

### Synthesis of **3a-c**

The synthesis of enantiomerically compounds **3b** and **3c** and their racemic mixture **3a** was achieved in 2 steps, as shown in the synthetic scheme shown in figure 2.

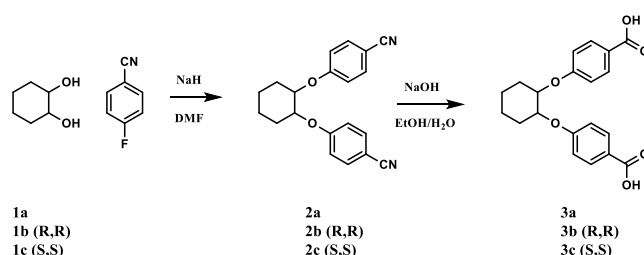


**Figure 2.** Synthetic pathway followed for the synthesis of the racemic mixture **3a** and enantiomerically pure ligands **3b** and **3c**.

Starting with either the racemic mixture of *trans*-1,2-cyclohexanediol **1a** or enantiomerically pure molecules (*R,R*)-*trans*-1,2-cyclohexanediol (**1b**) or (*S,S*)-*trans*-1,2-cyclohexanediol (**1c**), the condensation with 4-fluorobenzonitrile in DMF in the presence of NaH as base afforded the nitrile intermediate **2a** (74 %), **2b** (46 %) and **2c** (61 %) respectively. Their hydrolysis in  $EtOH/H_2O$  by NaOH led quantitatively to the targeted ligands **3a**, **3b** and **3c** (Figure 2). All three compounds **3a-c** were fully characterized in solution by common techniques and in the solid state by X ray diffraction on single crystals.

The enantiomerically pure ligands **3b** and **3c** were also characterized by CD spectroscopy in solution in  $CHCl_3$  (Figure 3).

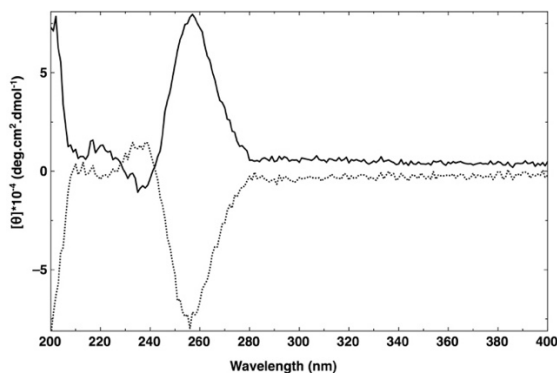


**Figure 3.** Circular Dichroism spectra of **3b** (black solid line) and **3c** (black dashed line) in  $\text{CHCl}_3$  at RT.

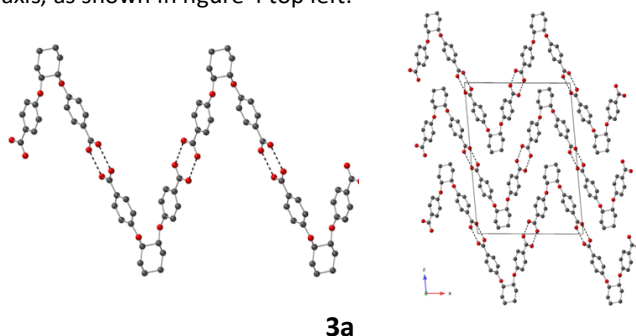
### Structures of **3a-c** in the solid-state

Crystals of **3a-c** have been obtained by slow vapor diffusion of MeOH into a  $\text{CHCl}_3$  solution containing the racemic mixture **3a** or the chiral ligands **3b** or **3c** (see experimental section). Whereas **3b** and **3c** crystallize in the monoclinic chiral space group  $P2_1$ , **3a**, as expected, crystallizes in the monoclinic achiral  $P2_1/c$  space group (see crystallographic table 1). In all three cases, crystals are composed of the organic ligands without any solvent molecules. Compounds **3a-c** are in their carboxylic form and thus behaves as self-complementary ligands forming H-bonded dimers.<sup>44</sup> Indeed, in all cases, a short ( $\text{C}=\text{O}$ ) and a long ( $\text{C}-\text{OH}$ ) bonds are observed (see table 2). The translation of carboxylic-carboxylic H-bonded nodes leads to the formation of 1D networks.

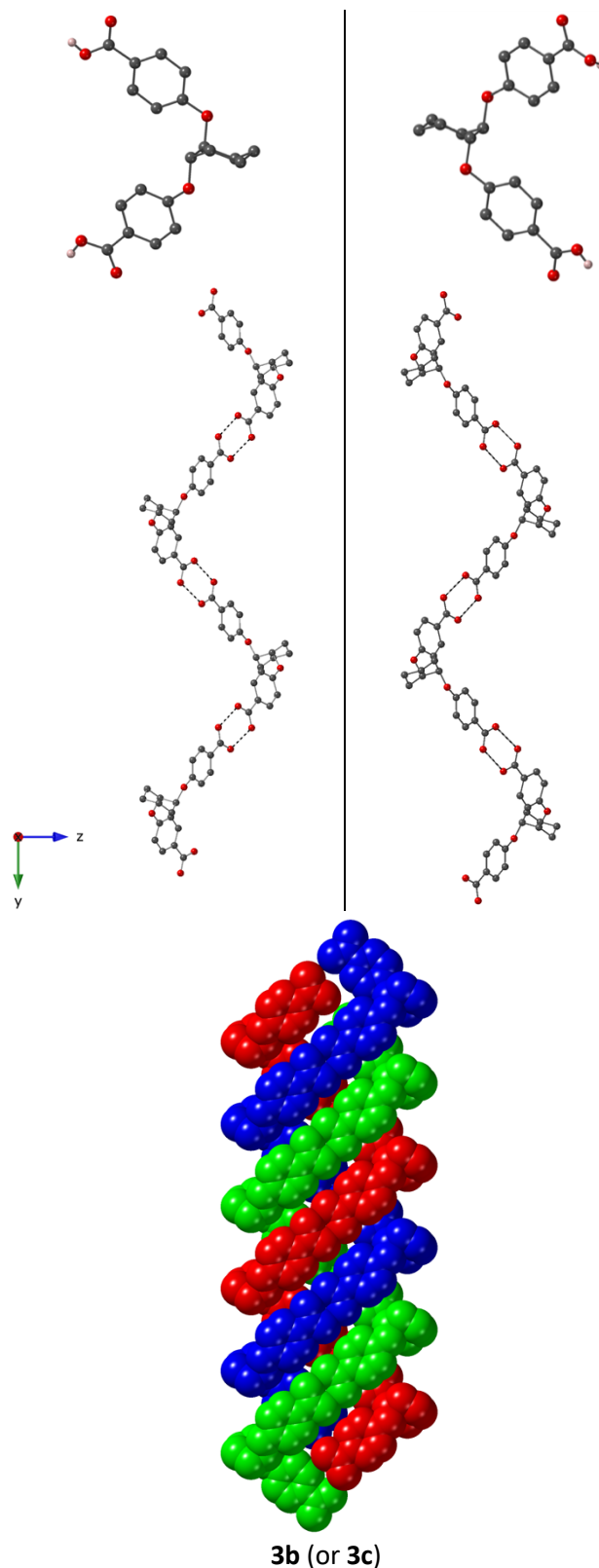
As expected, the partially flexible **3a-c** adopt a V-Shape with angles of  $69.5^\circ$  for **3b**,  $68.9^\circ$  for **3c** and  $46.8^\circ$  for **3a**. The angles and distances observed for **3a-c** in the crystalline phase are in agreement with those observed for benzoic acid and cyclohexanediol derivatives and thus will not be further commented here.

For the racemic mixture **3a**, composed of **3b** and **3c**, the formation of a zig-zag flat H-bonded chain running along the  $a$  axis is observed (figure 4 top left). Consecutive units possessing opposite chirality are interconnected by carboxylic/carboxylic interactions with O-O distances of 2.627(4) and 2.636(3) Å (see table 2).

In the crystal, the chains are superimposed along the  $b$  and  $c$  axis, as shown in figure 4 top left.



**3a**



**3b (or 3c)**

**Figure 4.** Representation of the H-bond assembled molecular networks based on self-complementary **3a-c** in the crystalline phase: racemic mixture **3a** displaying a zig-zag H bonded chain (top and middle), together with the corresponding packing; enantiomerically pure compounds **3b** and **3c** forming helical 1D H-bonded chains organized as triple helices (bottom). For description of architectures see text.

In marked contrast with the racemic mixture **3a**, enantiomerically pure compounds **3b** and **3c** lead to

isostructural crystals displaying opposite chirality. The translation of the carboxylic-carboxylic recognition motif (O-O distances of 2.583(3) and 2.622(3) Å for **3b** and 2.591(3) and 2.613(3) for **3c**, table 2) between consecutive units leads to the formation of helical chains (figure 4). The helicoidal H bonded networks form triple helices as shown in figure 4. The triple helices are packed in a parallel fashion in the xOz plane. O-H-O interactions are observed between two triple helices with an O-O distance of 3.182 (4) Å and 3.184 (4) Å for **3b** and **3c** respectively.

	<b>3a</b>	<b>3b</b>	<b>3c</b>
C-O (Å)	1.241(3)	1.258(4)	1.267(3)
	1.263(3)	1.268(3)	1.268(3)
	1.268(4)	1.271(3)	1.274(3)
	1.295(3)	1.276(3)	1.275(3)
O-O (Å)	2.627(4)	2.583(3)	2.591(3)
	2.636(3)	2.622(3)	2.613(3)

**Table 2.** Main distances and angles for **3a-c**.

The microcrystalline powders of the enantiomerically pure ligands **3b** and **3c** were also characterized by XRPD, showing the absence of crystallised racemic **3a** in the solid for both compounds. (see figure S1 in ESI)

As described above, enantiomerically pure compounds **3b** and **3c**, as well their racemic mixture **3a** in their protonated form, are self-complementary organic ligands leading to H-bonded networks.

### Coordination properties of **3b-c**

**3b** and **3c**, upon deprotonation offer two carboxylate coordination units and thus may be combined with metallic cations. For generating coordination networks, both chiral ligands **3b** and **3c** were combined with Cd(II) (as Cd(NO<sub>3</sub>)<sub>2</sub>) since cadmium in the oxidation state 2 favours the bidentate coordination mode of carboxylate bearing ligands.<sup>45,46</sup>

For the generation of Cd(II) coordination networks, ancillary N-donor ligand such as Dabco (1,4-Diazabicyclo[2.2.2]octane) or 4,4' bipyridine (bipy) have been used. The crystallization process was carried out under solvothermal conditions. It worth noting that, despite several attempts, it was not possible to obtain single crystals of coordination compound for the racemic mixture **3a**.

### Cd-Dabco derivatives

For **3b** and **3c**, isostructural crystals **Cd-3b-Dabco** and **Cd-3c-Dabco** (C<sub>20</sub>H<sub>18</sub>O<sub>6</sub>Cd(H<sub>2</sub>O)(C<sub>6</sub>H<sub>12</sub>N<sub>2</sub>) (see experimental section) were obtained and characterized by X-ray diffraction on single crystal. Both systems crystallize in an orthorhombic chiral space Group *P*<sub>2</sub><sub>1</sub><sub>2</sub><sub>1</sub><sub>2</sub> (table 3).

The crystal is composed of the chiral organic ligands **3b** (or **3c**), Cd<sup>2+</sup> cation, H<sub>2</sub>O molecule coordinated to the metallic

cation, and Dabco auxiliary ligands. The combination of the V-shape ligand (V angles of 50.1° and 50.4° for the **Cd-3b-Dabco** and **Cd-3c-Dabco** respectively) with Cd<sup>2+</sup> cation leads to the formation of a binuclear metallamacrocycle,<sup>47,48</sup> resulting from the bis-bidentate behaviour of ligands **3b** or **3c**. It is interesting to note, that in the coordination sphere of the metallic cation, a water molecule is also present.

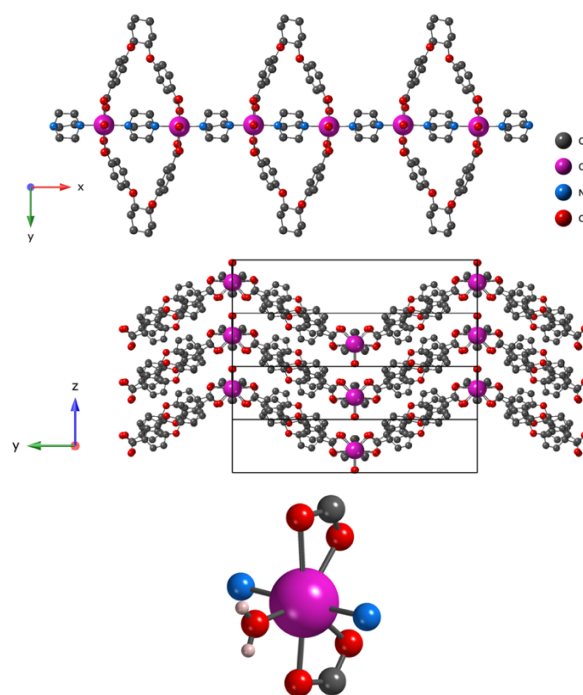


**Figure 5.** A portion of the chiral 1D coordination network obtained upon combining Cd(NO<sub>3</sub>)<sub>2</sub>, **3b** or **3c** and Dabco auxiliary ligand: metallamacrocycles connected by Dabco leading to a 1D chain along the *a* axis (top), together with the corresponding packing (middle); coordination sphere around the metal centre (bottom).

The similar C-O distances observed for **Cd-3b-Dabco** and **Cd-3c-Dabco** indicates that both ligands are in their carboxylate form (table 4). Cd(II) cations are hepta-coordinated and surrounded by two nitrogen atoms in *trans* disposition, belonging to different Dabco ligands, 2 carboxylate moieties acting as bidentate ligands and one water molecule (figure 5). In the structure, two types of ligand Dabco (one internal and one external) are present. Consecutive metallamacrocycles are linked by external Dabco molecules, leading to a 1D coordination network running along the *a* axis (figure 5). The distance between two consecutive Cd cations belonging to the same network varies between 7.209(5) and 7.342(5) Å. The 1D chains are stacked along the *a* and *b* axis (figure 5).

	<b>Cd-3b-Dabco</b>	<b>Cd-3c-Dabco</b>	<b>Cd-3b-Bipy</b>	<b>Cd-3c-Bipy</b>
C-O	1.238(3)	1.239(3)	1.253(6)	1.24(2)
	1.259(3)	1.259(3)	1.255(6)	1.242(17)
	1.264(3)	1.265(3)	1.261(5)	1.287(17)
	1.282(2)	1.284(3)	1.262(5)	1.288(18)
Cd-O	2.2981(14)	2.3000(16)	2.335(3)	2.297(8)
	2.3789(14)	2.3847(15)	2.380(3)	2.321(10)
	2.4533(16)	2.4544(18)	2.386(3)	2.382(11)
	2.6723(15)	2.6755(18)	2.378 (3)	2.390(14)
			2.518(3)	2.556(9)



Cd-O <sub>w</sub>	2.2830(14)	2.2869(18)	-	-
Cd-N	2.3187(17)	2.3186(18)	2.299(3)	2.307(9)
	2.3744(18)	2.3748(19)	2.332(4)	2.332(9)
Cd-Cd	7.209(5) and 7.342(5)	7.211(5) and 7.342(5)	3.830(3)	3.823(4)

Table 4 : Main distances for **Cd-3b-Dabco**, **Cd-3c-Dabco**, **Cd-3b-Bipy** and **Cd-3c-Bipy**

The purity of the **Cd-3b-Dabco** and **Cd-3c-Dabco** phases was investigated by PXRD on microcrystalline powder. For both compounds, a good match between the observed and simulated patterns from the XRD data was obtained (figure 6).

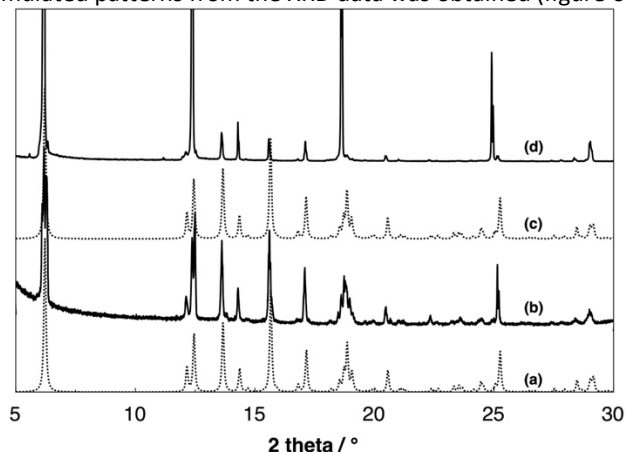


**Figure 6.** Comparison of the simulated XRPD diagrams ((a) for **Cd-3b-Dabco** and (c) for **Cd-3c-Dabco**) and recorded ((b) for **Cd-3b-Dabco** and (d) for **Cd-3c-Dabco**). Discrepancies in intensity between the observed and simulated patterns are due to preferential orientations of the microcrystalline powders.

### Cd-Bipyridine derivatives

The combination of **3b** or **3c** with Cd<sup>2+</sup> cation in the presence of 4,4'-bipyridine again affords two isostructural crystals **Cd-3b-Bipy** and **Cd-3c-Bipy** (C<sub>20</sub>H<sub>18</sub>O<sub>6</sub>Cd(C<sub>10</sub>H<sub>8</sub>N<sub>2</sub>)) under solvothermal conditions (see experimental part). Both compounds crystallize in a monoclinic chiral space Group *C*2. The crystal contains **3b** (or **3c**) chiral organic V-shape ligands (angles of 21.3° and 21.4° for the **Cd-3b-Bipy** and **Cd-3c-Bipy** respectively), Cd<sup>2+</sup> cation and the Bipy ancillary ligand (figure 7). Due to the presence of disordered solvent molecules in the crystal, the structures were refined by applying the squeeze command.<sup>49</sup> A thick 2D architecture, with a metallic plane encapsulated in the V shape organic ligands, resulting from the formation of Cd-dimeric units is observed (figure 7, middle). The 4,4'-bipy ligands behave as pillars between the bimetallic nodes. Within the coordination network, the Cd-Cd distances are equal to 3.830(3) and 3.823(4) Å for **Cd-3b-Bipy** and **Cd-3c-Bipy**, respectively. This corresponds to what is usually observed for Cd(II) carboxylate bridged dinuclear units.<sup>50</sup> The bulky 2D system, parallel to the xOy planes, are formed by bridging of dinuclear metallic units, along the c axis, by the V shape ligands **3b** or **3c** and by linear 4,4' bipyridine ligands in the *b* direction (figure 7 top).

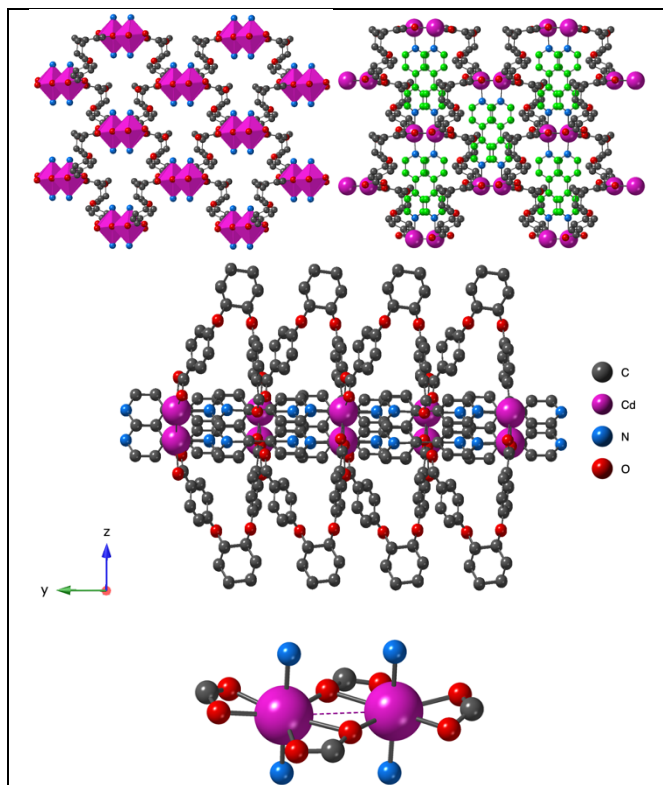


**Figure 7.** A portion of the chiral Cd 2D coordination network formed upon combination of Cd(NO<sub>3</sub>)<sub>2</sub>, **3b-c** and bipy (represented in green) in the xOy plane: top, the thick 2D- in the yOz plane (middle); the coordination sphere around the binuclear nodes (bottom).

Again, similar C-O distances for **Cd-3b-Bipy** and **Cd-3c-Bipy** indicate the deprotonation of ligands **3b** or **3c** (table 4). The metallic centers are, as in the previous cases, hepta-coordinated and surrounded by two nitrogen atoms in *trans* position, belonging to 4,4' bipy ligands, three carboxylate moieties, one acting as a bidentate unit and the other two as bridges between the dimeric unit (figure 7). The bond distances around the metallic centres are reported in table 4.

The 2D arrays are stacked along the *c* axis, some van der Waals contacts between ligands belonging to two adjacent planes are observed.

The purity of **Cd-3b-Bipy** and **Cd-3c-Bipy** phases was studied by PXRD on microcrystalline powder (figure 8) which revealed a good match between the recorded and the simulated pattern using XRD data.

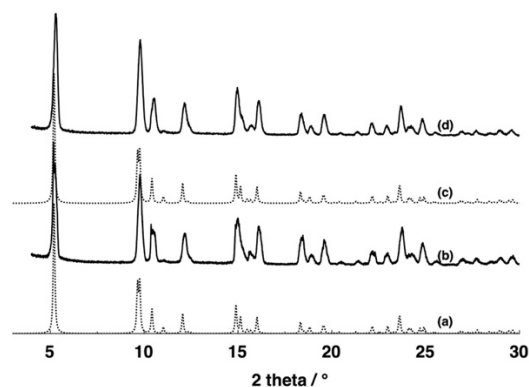


**Figure 8.** Comparison of the simulated XRPD diagrams ((a) for **Cd-3b-Bipy** and (c) for **Cd-3c-Bipy**) and recorded ((b) for **Cd-3b-Bipy** and (d) for **Cd-3c-Bipy**). Discrepancies in intensity between the observed and simulated patterns are due to preferential orientations of the microcrystalline powders.

## Conclusions

The synthesis of two enantiomerically pure compounds **3b** and **3c** and their racemic mixture **3a**, that are based on the (*trans*-1,2-cyclohexanediol bearing two benzoic groups, was achieved. The solid-state structures of these flexible V-shape dicarboxylic connectors was investigated by X-ray diffraction on single crystal. Owing to the self-complementary nature of the ligands resulting from the recognition of carboxylic sites, all three compounds lead to the formation of zigzag 1D H-bonded networks. As expected, crystals of the racemic mixture are achiral whereas the two enantiomerically pure ligands **3b** and **3c**, afford isostructural helical 1D networks with opposite handedness, organized in triple helical architectures.

Interestingly, the chiral ligands **3b** and **3c** in their deprotonated form lead, under solvothermal conditions, to the

formation of coordination networks when combined with  $\text{Cd}^{2+}$  cation in the presence of N donor ancillary ligands such as Dabco (**Cd-3b-Dabco** and **Cd-3c-Dabco**) or 4,4' Bipy (**Cd-3b-Bipy** and **Cd-3c-Bipy**) behaving as linear connectors. Chiral crystals of **Cd-3b-Dabco** and **Cd-3c-Dabco** are composed of 1D networks resulting from the interconnection of consecutive metallamacrocycles by bis monodentate Dabco, whereas in the case of **Cd-3b-Bipy** and **Cd-3c-Bipy**, a 2D network resulting from the interconnection of binuclear  $\text{Cd}(\text{II})$  nodes by the chiral and ancillary ligands.

The formation of other enantiomerically pure coordination polymers using other metals is currently under investigation.

## Conflicts of interest

There are no conflicts to declare.

## Acknowledgements

We thank the University of Strasbourg, the C.N.R.S, the International centre for Frontier Research in Chemistry (icFRC), the Labex CSC (ANR-10-LABX-0026 CSC) within the Investissement d'Avenir program ANR-10-IDEX-0002-02, the Ministère de l'Enseignement Supérieur et de la Recherche for financial support.

## Notes and references

1. K. Kim, M. Banerjee, M. Yoon and S. Das, in *Topics in Current Chemistry*, ed. M. Schröder, Springer, Berlin Heidelberg, 2010, ch. 7, **293**, 115-153.
2. W. Lin, *Top. Catal.*, 2010, **53**, 869-875.
3. L. Ma and W. Lin, in *Topics in Current Chemistry*, ed. M. Schröder, Springer, Berlin Heidelberg, 2010, ch. 7, **293**, 175-205.
4. R. E. Morris and X. Bu, *Nat. Chem.*, 2010, **2**, 353-361.
5. K. K. Bisht, B. Parmar, Y. Rachuri, A. C. Kathalikattil and E. Suresh, *CrystEngComm*, 2015, **17**, 5341-5356.
6. B. F. Abrahams, B. F. Hoskins and R. Robson, *J. Am. Chem. Soc.*, 1991, **113**, 3606-3607.
7. M. W. Hosseini, *Acc. Chem. Res.*, 2005, **38**, 313-323.
8. M. W. Hosseini, *CrystEngComm*, 2004, **6**, 318-322.
9. *Chem. Rev.*, 2012, **112**, MOFs special issue.
10. *Chem. Soc. Rev.*, 2014, **43**, themed issue on MOFs.
11. E. V. Anokhina, Y. B. Go, Y. Lee, T. Vogt and A. J. Jacobson, *J. Am. Chem. Soc.*, 2006, **128**, 9957-9962.
12. R. Vaidhyanathan, D. Bradshaw, J. N. Rebilly, J. P. Barrio, J. A. Gould, N. G. Berry and M. J. Rosseinsky, *Angew. Chem. Int. Ed.*, 2006, **45**, 6495-6499.
13. W. Xuan, M. Zhang, Y. Liu, Z. Chen and Y. Cui, *J. Am. Chem. Soc.*, 2012, **134**, 6904-6907.
14. R. E. Morris, *Chem. Commun.*, 2009, 2990-2998.
15. X.-L. Tong, T.-L. Hu, J.-P. Zhao, Y.-K. Wang, H. Zhang and X.-H. Bu, *Chem. Commun.*, 2010, **46**, 8543-8545.
16. Q.-Y. Liu, Y.-L. Wang, N. Zhang, Y.-L. Jiang, J.-J. Wei and F. Luo, *Cryst. Growth Des.*, 2011, **11**, 3717-3720.
17. X. Tan, J. Zhan, J. Zhang, L. Jiang, M. Pan and C.-Y. Su, *CrystEngComm*, 2012, **14**, 63-66.
18. L. Dong, W. Chu, Q. Zhu and R. Huang, *Cryst. Growth Des.*, 2011, **11**, 93-99.
19. P. Larpent, A. Jouaiti, N. Kyritsakas and M. W. Hosseini, *Dalton Trans.*, 2014, **43**, 166-172.
20. J. Chen and F. M. MacDonnell, *Chem. Commun.*, 1999, 2529-2530.
21. S. J. Garibay, J. R. Stork, Z. Wang, S. M. Cohen and S. G. Telfer, *Chem. Commun.*, 2007, 4881-4883.
22. C. Xu, A. Guenet, N. Kyritsakas, J.-M. Planeix and M. W. Hosseini, *Inorg. Chem.*, 2015, **54**, 10429-10439.
23. Z.-H. Yan, D. Li and X.-B. Yin, *Sci. Bull.*, 2017, **62**, 1344-1354.
24. M. Enamullah, V. Vasylyeva, M. A. Quddus, M. K. Islam, S.-P. Höfert and C. Janiak, *CrystEngComm*, 2018, **20**, 4724-4734.
25. J. S. Seo, D. Whang, H. Lee, S. I. Jun, J. Oh, Y. J. Jeon and K. Kim, *Nature*, 2000, **404**, 982-986.
26. Y. Peng, T. Gong, K. Zhang, X. Lin, Y. Liu, J. Jiang and Y. Cui, *Nat. Commun.*, 2014, **5**, 4406.



27. T. Sawano, N. C. Thacker, Z. Lin, A. R. McIsaac and W. Lin, *J. Am. Chem. Soc.*, 2015, **137**, 12241-12248.
28. D. Asnaghi, R. Corso, P. Larpent, I. Bassanetti, A. Jouaiti, N. Kyritsakas, A. Comotti, P. Sozzani and M. W. Hosseini, *Chem. Commun.*, 2017, **53**, 5740-5743.
29. J. Guo, Y. Zhang, Y. Zhu, C. Long, M. Zhao, M. He, X. Zhang, J. Lv, B. Han and Z. Tang, *Angew. Chem.*, 2018, **130**, 6989-6993.
30. X. Han, J. Huang, C. Yuan, Y. Liu and Y. Cui, *J. Am. Chem. Soc.*, 2018, **140**, 892-895.
31. S. Das, S. Xu, T. Ben and S. Qiu, *Angew. Chem. Int. Ed.* 2018, **57**, 8629-8633.
32. L. Ma, C. Abney and W. Lin, *Chem. Soc. Rev.*, 2009, **38**, 1248-1256.
33. L. Ma, J. M. Falkowski, C. Abney and W. Lin, *Nat. Chem.*, 2010, **2**, 838-846.
34. M. Yoon, R. Srirambalaji and K. Kim, *Chem. Rev.*, 2012, **112**, 1196-1231.
35. M. M. Wanderley, C. Wang, C.-D. Wu and W. Lin, *J. Am. Chem. Soc.*, 2012, **134**, 9050-9053.
36. D. Sun, Y. Ke, D. J. Collins, G. A. Lorigan and H.-C. Zhou, *Inorg. Chem.*, 2007, **46**, 2725-2734.
37. D. N. Dybtsev, M. P. Yutkin, E. V. Peresypkina, A. V. Virovets, C. Serre, G. Férey and V. P. Fedin, *Inorg. Chem.*, 2007, **46**, 6843-6845.
38. W. J. Rieter, K. M. Pott, K. M. Taylor and W. Lin, *J. Am. Chem. Soc.*, 2008, **130**, 11584-11585.
39. Y. Liu, W. Xuan and Y. Cui, *Adv. Mater.*, 2010, **22**, 4112-4135.
40. Q. Zhu, T. Sheng, R. Fu, C. Tan, S. Hu and X. Wu, *Chem. Commun.*, 2010, **46**, 9001-9003.
41. S. R. Batten, S. M. Neville and D. R. Turner, in *Coordination Polymers: Design, Analysis and Application*, The Royal Society of Chemistry, Cambridge, 2009.
42. M.-J. Lin, A. Jouaiti, P. Grosshans, N. Kyritsakas and M. W. Hosseini, *Chem. Commun.*, 2011, **47**, 7635-7637.
43. G. M. Sheldrick, Program for Crystal Structure Solution, University of Göttingen, Göttingen, Germany, 1997.
44. T. Steiner *Angew. Chem. Int. Ed.* 2002, **41**, 48-76.
45. M.-D. Zhang, Y. Jiao, J. Li and M.-D. Chen *Mendeleev Commun.*, 2015, **25**, 65-66.
46. L. Wang, M. Yang, G. Li, Z. Shi and S. Feng *Inorg. Chem.*, 2006, **45**, 2474-2478.
47. A. W. Maverick, S.C. Buckingham, Q. Yao, J. R. Bradbury and G. G. Stanley, *J. Am. Chem. Soc.* 1986, **108**, 743-748.
48. C. H. M. Amijs, G. P. M. v. Klink and G. v. Koten, *Dalton Trans.*, 2006, 308-327.
49. A. L. Spek, *J. Appl. Crystallogr.*, **2003**, **36**, 7-13.
50. S. Shit, J. Chakraborty, B. Samanta, G. Pilet and S. Mitra, *J. Mol. Struct.*, 2009, **919**, 361-365.

## ARTICLE

**Table 1.** Crystallographic parameters for **3a-c** recorded at 173 K.

	<b>3a</b>	<b>3b</b>	<b>3c</b>
	Racemate	(R,R)	(S,S)
Empirical formula	C <sub>20</sub> H <sub>20</sub> O <sub>6</sub>	C <sub>20</sub> H <sub>20</sub> O <sub>6</sub>	C <sub>20</sub> H <sub>20</sub> O <sub>6</sub>
Formula weight g/mol	356.36	356.36	356.36
Crystal system	Monoclinic	Monoclinic	Monoclinic
Space group	P 21/c	P 21	P 21
a(Å)	15.001(2)	9.2808(5)	9.2536(5)
b(Å)	5.5536(5)	7.6511(3)	7.6512(3)
c(Å)	21.455(3)	12.6946(6)	12.6769(7)
α(deg)	90	90	90
β(deg)	95.230(2)	108.142(2)	108.093(2)
γ(deg)	90	90	90
V(Å <sup>3</sup> )	1780.0(4)	856.61(7)	853.16(7)
Z	4	2	2
Colour	white	white	white
Crystal dim (mm)	0.120 x 0.060 x 0.060	0.070 x 0.060 x 0.050	0.060 x 0.050 x 0.050
Dcalc (gcm <sup>-3</sup> )	1.330	1.382	1.387
F(000)	752	376	376
μ (mm <sup>-1</sup> )	0.098	0.102	0.103
Wavelength (Å)	0.71073	0.71073	0.71073
Reflections collected	10173	7396	8761
Independent reflections	3816 [R(int) = 0.0415]	3730 [R(int) = 0.0236]	4095 [R(int) = 0.0255]
Final R indices [I>2σ(I)]	R1 = 0.0562, wR2 = 0.1480	R1 = 0.0401, wR2 = 0.1164	R1 = 0.0451, wR2 = 0.0756
R indices (all data)	R1 = 0.1321, wR2 = 0.1973	R1 = 0.0464, wR2 = 0.1201	R1 = 0.0539, wR2 = 0.0773
Goodness-of-fit on F <sup>2</sup>	1.014	1.060	1.719
Largest diff. peak / hole (eÅ <sup>-3</sup> )	0.163 and -0.208	0.359 and -0.292	0.249 and -0.254

**Table 3.** Crystallographic parameters for **Cd-3b-Dabco**, **Cd-3c-Dabco**, **Cd-3b-Bipy** and **Cd-3c-Bipy** recorded at 173 K

	<b>Cd-3b-Dabco</b>	<b>Cd-3c-Dabco</b>	<b>Cd-3b-Bipy</b>	<b>Cd-3c-Bipy</b>
	(R,R)	(S,S)	(R,R)	(S,S)
Empirical formula	C <sub>26</sub> H <sub>32</sub> CdN <sub>2</sub> O <sub>7</sub>	C <sub>26</sub> H <sub>32</sub> CdN <sub>2</sub> O <sub>7</sub>	C <sub>30</sub> H <sub>26</sub> CdN <sub>2</sub> O <sub>6</sub>	C <sub>30</sub> H <sub>26</sub> CdN <sub>2</sub> O <sub>6</sub>
Formula weight g/mol	596.93	596.93	622.93	622.93
Crystal system	Orthorhombic	Orthorhombic	Monoclinic	Monoclinic
Space group	P 21 21 2	P 21 21 2	C 2	C 2
a(Å)	14.5475(6)	14.5483(5)	16.0435(14)	15.6883(18)
b(Å)	28.4089(12)	28.4278(12)	11.6969(8)	11.7144(12)
c(Å)	6.1616(3)	6.1660(2)	18.4980(15)	17.7770(18)
α(deg)	90	90	90	90
β(deg)	90	90	113.454(2)	109.199(3)
γ(deg)	90	90	90	90
V(Å <sup>3</sup> )	2546.46(19)	2550.11(16)	3184.5(4)	3085.3(6)
Z	4	4	4	4
Colour	white	white	white	white
Crystal dim (mm)	0.120 × 0.120 × 0.100	0.080 × 0.070 × 0.070	0.090 × 0.080 × 0.080	0.040 × 0.040 × 0.040
D <sub>calc</sub> (gcm <sup>-3</sup> )	1.557	1.555	1.299	1.341
F(000)	1224	1224	1264	1264
μ (mm <sup>-1</sup> )	0.906	0.904	0.725	0.749
Wavelength (Å)	0.71073	0.71073	0.71073	0.71073
Reflections collected	146392	37014	19760	5664
Independent reflections	7046 [R(int) = 0.0331]	7439 [R(int) = 0.0315]	8357 [R(int) = 0.0429]	5140 [R(int) = 0.0355]
Final R indices [I>2σ(I)]	R1 = 0.0204, wR2 = 0.0485	R1 = 0.0245, wR2 = 0.0559	R1 = 0.0426, wR2 = 0.0897	R1 = 0.1084, wR2 = 0.2562
R indices (all data)	R1 = 0.0215, wR2 = 0.0491	R1 = 0.0309, wR2 = 0.0589	R1 = 0.0572, wR2 = 0.0959	R1 = 0.1708, wR2 = 0.3170
Goodness-of-fit on F <sup>2</sup>	1.094	0.971	1.031	1.085
Largest diff. peak / hole (eÅ <sup>-3</sup> )	0.496 and -0.711	0.353 and -0.336	1.458 and -1.092	1.787 and -1.525
Flack parameter	-0.012(4)	-0.018(9)	-0.009(16)	0.04(10)

## Graphical Abstract

